n-HEPTANE-AIR COUNTERFLOW DIFFUSION FLAME: RATE-RATIO ASYMPTOTIC ANALYSIS

Fachini F.F.- fachini@yabae.cptec.inpe.br
Instituto Nacional de Pesquisas Espaciais,
12630-000, Cachoeira Pta - SP, Brazil.

Williams F.A. - faw@ames.ucsd.edu
Seshadri K. - seshadri@cauvery.ucsd.edu
Mechanical and Aerospace Engineering Department
Center for Combustion and Energy Research,
University of California, San Diego,
La Jolla CA 92093, USA.

Abstract. *The method of rate-ratio assympotics is employed in the analysis of a n-heptane counterflow diffusion flame to specify the extinction conditions. The oxidation of the n-heptane is represented by a mechanism of four-global reactions. The first reaction describes the attack of the fuel by the H-radical and the other three reactions correspond to the oxidation of CO and H_2, and are the same reactions found in the oxidation of methane. The counterflow configuration imposes a stretch on the flame, which can lead to extinction. Extinction is observed for low values of stretch when radiative energy loss is large and for high values of stretch because reaction is incomplete. The results show flame extinction for low and high stretch levels and the conditions for no existence of flames.*

Keywords:. Diffusion Flame, Extinction, Rate-Ratio Asymptotics, n-Heptane.

1. INTRODUCTION

Flames stabilized around the stagnation point of a counterflow have been extensively studied because they are the closest representation of flamelets which are employed to describe locally the behavior of flames in both unpremixed and premixed turbulent combustion (Tsuji, 1982; Law, 1988; Dixon-Lewis, 1990). In spite of a lot of attention on these flames, there are features that have not been analysed yet From the rate-ratio asymptotic optics, this analysis addresses the effects of the H-radical in the fuel breaking reaction and the effects of radiative energy loss on the extinction process of the n-heptane diffusion flame.

The rate-ratio asymptotics method, which handles with more than one global reaction, is formulated considering two main assumptions: First, the chemical reaction is given by a very reduced numbers of steps: in the first step the H-radical attacks the fuel to form CO and H_2 and in the other steps the oxidation of these species (Peters and Williams, 1987). Second, each reaction occurs in a very distintic rate, so that the layers where the reactions proceed have different thicknesses, so that it is possible to treat the processes inside each layer almost isolatedly. The reaction between n-heptane and H-radical occurs in the first layer on the fuel side of the flame and this is the thinnest layer. The oxidation of H_2 and the generation of H-radical take place in the thickest layer, called the oxidation layer, on the oxidante side of the flame. Between these two layer there is another one where the reaction between CO and H_2O occurs and its thickness is larger than the fuel breaking layer and smaller than the oxidation layer

Since the n-heptane is a pure substance and represents well the gasoline, it has been extensively used in experimental, numerical and theoretical analysis. However, contrarily to light hydrocarbons, the oxidation of heavy hydrocarbons, like n-heptane, occurs by a great number of routes, a fact that makes difficult to find a reduced kinetic mechanism representative of the complete chemical reaction. A signal of the difficulties on specifying a reduced mechanism can be seen in the discrepancy on the number of moles of H-radical species consumed in the first reaction considered by the models. There are models with four-global steps for n-heptane oxidation that consider 10 moles of H-radical (Card and Williams, 1992; Card, 1992; Card, 1993) and other models that consider 2 moles of H-radical (Bollig et all, 1996).

In the counterflow configuration flames extinguish for low and high values of stretch. For low stretch the radiative energy loss is responsible for flame extinction (T'ien, 1986; Olson and T'ein, 1987) For high stretch the extinction occurs due to incomplete combustion (Liñán, 1974; Puri and Seshadri, 1986;Seshadri and Peters, 1988; Bui-Pham and Seshadri, 1991) . Here we analise the influence of the H-radical on the extinction process of the counterflow n-heptane diffusion flames in both limits

2. REDUCED KINETIC MECHANISM FOR N-HEPTANE OXIDATION

In this analysis the systematic procedure to determine the number of moles of H-radical α is not followed. The value of α is a free parameter in the model. As it will be seen next, the flame structure depends on the reciprocal value of α, so that decreasing the value of α the diffusion flame becomes stronges and, consequently, the extinction occurs for higher value of stretch.

It is assumed that the reduced kinetic mechanism for the oxidation of the n-heptane

is given by the following four global reactions:

$$\begin{array}{rcll} C_7H_{16} + \alpha H + 7H_2O & \rightarrow & 7CO + \alpha_1 H_2 & Q_I \quad (I) \\ CO + H_2O & \rightarrow & CO_2 + H_2 & Q_{II} \quad (II) \\ H + H + M & \rightarrow & H_2 + M & Q_{III} \quad (III) \\ O_2 + 3H_2 & \rightarrow & 2H_2O + 2H & Q_{IV} \quad (IV) \end{array}$$

where $\alpha_1 = 15 + \alpha/2$, $Q_I = 1114.81 - 218.16\alpha$ $Q_{II} = 40.79$, $Q_{III} = -437.2$, and $Q_{IV} = -48.28$ kJ/mol. Notice that, for $\alpha < 5.09$, the first reaction is endothermic. Moreover, the reaction rates for reactions (I), (II), (III) and (IV) are

$$\begin{array}{rcl} w_I & = & w_{R2} + w_{R3} + w_{R4} + w_{R5} \\ w_{II} & = & w_{9f} - w_{9b} \\ w_{III} & = & w_5 \\ w_{IV} & = & w_{1f} - w_{1b} \end{array} \tag{1}$$

which are specified by the mechanism presented in the table 1.

Table 1: Chemical Kinetic Mechanism [1 - Seshadri and Peters, 1990; 2 - Li and Williams, 1999]

Number	*Reaction*	A_n	n_n	E_n
$1f$[1]	$O_2 + H \rightarrow OH + O$	2.000×10^{14}	0.00	70.338
$1b$[1]	$OH + O \rightarrow O_2 + H$	1.575×10^{13}	0.00	2.888
$2f$[1]	$H_2 + O \rightarrow OH + H$	1.800×10^{10}	1.00	36.952
$2b$[1]	$OH + H \rightarrow H_2 + O$	8.000×10^{9}	1.00	28.302
$3f$[1]	$H_2 + OH \rightarrow H_2O + H$	1.170×10^{9}	1.30	15.181
$3b$[1]	$H_2O + H \rightarrow H_2 + OH$	5.090×10^{9}	1.30	77.824
$4f$[1]	$OH + OH \rightarrow H_2O + O$	6.000×10^{8}	1.30	0
$4b$[1]	$H_2O + O \rightarrow OH + OH$	5.900×10^{9}	1.30	71.297
5[1]	$H + O_2 + M \rightarrow HO_2 + M$	2.300×10^{18}	−0.80	0
$9f$[1]	$CO + OH \rightarrow CO_2 + H$	1.510×10^{7}	1.30	−3.173
$9b$[1]	$CO_2 + H \rightarrow CO + OH$	1.570×10^{9}	1.30	93.520
$R2$[2]	$n - C_7H_{16} + H \rightarrow H_2 + C_3H_6 + C_2H_4 + C_2H_5$	2.600×10^{6}	2.40	18.700
$R3$[2]	$n - C_7H_{16} + H \rightarrow H_2 + C_4H_8 + C_2H_4 + CH_3$	2.080×10^{6}	2.40	18.700
$R4$[2]	$n - C_7H_{16} + H \rightarrow H_2 + 3C_2H_4 + CH_3$	1.320×10^{6}	2.54	28.300
$R5$[2]	$n - C_7H_{16} + H \rightarrow H_2 + C_5H_{10} + C_2H_5$	1.300×10^{6}	2.40	18.700

As it was done by Seshadri and Peters (1990), the radicals O and OH is assumed in steady state and the concentration of O-radical can be determined by

$$C_O = \frac{k_{1f} C_H C_{O_2} + \gamma(k_{2b} + \gamma k_{4f}) C_H^2}{(k_{2f} + \gamma K_3 k_{4b}) C_{H_2} + \gamma k_{1b} C_H}, \tag{2}$$

and assuming partial equilibrium for reaction 3, the concentration of OH-radical can be determined as a function of the H-radical concentration:

$$C_{OH} = \gamma C_H, \tag{3}$$

where $\gamma = C_{H_2O}/(K_3 C_{H_2})$ and $K_3 = k_{3f}/k_{3b}$.

However, imposing the partial equilibrium on reaction 2 and taking into account Eq.(3), the O-radical concentration can be determined as (Bai and Seshadri, 1999)

$$C_O = \frac{C_{H_2O} C_H^2}{K_2 K_3 C_{H_2}^2} \tag{4}$$

The concentration of the third body C_M appearing in reaction (III) is given by

$$C_M = \frac{p\bar{W}}{\hat{R}T} \sum_{i=1}^{N} \frac{\eta_i Y_i}{W_i} \tag{5}$$

where $\hat{R} = 82.05\text{atm}/(\text{cm}^3 \text{ mole K})$, W_i, η_i, and Y_i are the molecular weight, the catalytic efficiency, and the mass fraction of molecule i $(i = 1, \cdots, N)$, respectively.

3. MATHEMATICAL MODEL

The geometrical configuration of the counterflow associated with the assumption of boundary layer approximation around the stagnation point leads to the solution of the hydrodynamic problem as following (Keyes and Smooke, 1987; Kee at all, 1988; Libby and Smooke, 1997; Libby, 1998):

$$u/v_0 = (r/l)U(z), \quad \rho v/\rho_0 v_0 = V(z), \quad p/\rho_0 v_0^2 = P(z) - (r/l)^2 J/2 \tag{6}$$

where r, z,u, v, ρ, p, and J are respectively the radial coordinate, the axial coordinate nondimensionalized with the distance l between nozzles, the radial and axial component of the velocity, density, pressure, and a constant. The subscript 0 denotes the value of the variable at the nozzle located at $z = 0$ from where the oxidant stream comes, such that Y_{O_20} is the oxygen mass fraction and $1 - Y_{O_20}$ is the nitrogen mass fraction. The subscript 1 that will appear next specifies the value of the variable at the nozzle located at $z = 1$ from where the fuel stream comes, such that Y_{F1} is the fuel mass fraction and $1 - Y_{F1}$ is nitrogen mass fraction.

The radiative energy transfer is included in the model by the approximation of optically thin transparent gas and released in the CO_2 and H_2O bands. The Planck-mean absorption lengths for CO_2 and H_2O, $l_{P\ CO_2}$ and $l_{P\ H_2O}$, respectively, are taken from Rightley and Williams' analysis. (Rightley and Williams, 1997).

Taking Eqs. (6) into the conservation equations of mass and momentum and applying the approximation of boundary layer on the conservation equations of energy and species for the counterflow configuration, the following system of equations are found

$$\frac{dV}{dz} + 2\rho U = 0 \tag{7}$$

$$\rho U^2 + V\frac{dU}{dz} - \frac{d}{dz}\left(\frac{Pr}{Pe}\theta^n \frac{dU}{dz}\right) = J \tag{8}$$

$$V\frac{d\theta}{dz} - \frac{d}{dz}\left(\frac{\theta^n}{Pe}\frac{d\theta}{dz}\right) = q\sum_{i=I}^{IV} q_i w_i - \sigma\theta^4\left(X_{CO_2}\frac{\bar{l}_P}{l_{P\ CO_2}} + X_{H_2O}\frac{\bar{l}_P}{l_{P\ H_2O}}\right) \tag{9}$$

$$V\frac{dX_F}{dz} - \frac{d}{dz}\left(\frac{\theta^n}{PeL_F}\frac{dX_F}{dz}\right) = -w_I \tag{10}$$

$$V\frac{dX_{O_2}}{dz} - \frac{d}{dz}\left(\frac{\theta^n}{PeL_{O_2}}\frac{dX_{O_2}}{dz}\right) = -w_{IV} \tag{11}$$

$$V\frac{dX_{H_2}}{dz} - \frac{d}{dz}\left(\frac{\theta^n}{PeL_{H_2}}\frac{dX_{H_2}}{dz}\right) = \alpha_1 w_I + w_{II} + w_{III} - 3w_{IV} \tag{12}$$

$$V\frac{dX_H}{dz} - \frac{d}{dz}\left(\frac{\theta^n}{PeL_H}\frac{dX_H}{dz}\right) = -\alpha w_I - 2w_{III} + 2w_{IV} \tag{13}$$

$$V\frac{dX_{H_2O}}{dz} - \frac{d}{dz}\left(\frac{\theta^n}{PeL_{H_2O}}\frac{dX_{H_2O}}{dz}\right) = -7w_I - 2w_{II} + 2w_{IV} \tag{14}$$

$$V\frac{dX_{CO}}{dz} - \frac{d}{dz}\left(\frac{\theta^n}{PeL_{CO}}\frac{dX_{CO}}{dz}\right) = -7w_I - w_{II} \tag{15}$$

$$V\frac{dX_{CO_2}}{dz} - \frac{d}{dz}\left(\frac{\theta^n}{PeL_{CO_2}}\frac{dX_{CO_2}}{dz}\right) = w_{II} \tag{16}$$

where θ is the temperature nondimensionalized by the temperature of the oxidant stream at $z = 0$ and X_i is the modified mass fraction defined as $Y_i W_{N_2}/W_i$; W_i is the molecular weight of species i, $i = F,\ O_2,\ N_2,\ H_2,\ H,\ H_2O,\ CO,\ CO_2$. The parameter $q = Q/c_pT_0$ is the nondimensionalized total heat released by the one step global reaction and the value of Q is determined by $Q_I + 7Q_{II} + (11 - \alpha/2)Q_{III} + 11Q_{IV}$, and $q_i = Q_i/Q$ for $i = I, ..., IV$. The nondimensionalized emissivity σ appearing in the energy conservation equation is defined as

$$\sigma = \frac{4\sigma_B T_0^3 l}{\bar{l}_P c_p \rho_0 v_0}$$

where σ_B is the Stefan-Boltzmann constant and $\bar{l}_{Pi}$ is the mean value between $l_{P\ CO_2}$ and $l_{P\ H_2O}$ evaluated at the flame position. Pe, Pr, and L_i are the Peclet, Prandlt, and Lewis numbers, respectively, and are defined as

$$Pe = \frac{lv_0}{k_0/(\rho_0 c_p)}, \quad Pr = \frac{\mu_0}{k_0/c_p}, \quad L_i = \frac{k_0/(\rho_0 c_p)}{D_{i0}}$$

where c_p, k, D_i, and μ are, respectively, the specific heat at constant pressure (assumed constant), thermal conductivity, diffusion coefficient, and coefficient of viscosity, which depend only on temperature:

$$\frac{\rho D_i}{\rho_0 D_{i0}} = \frac{k}{k_0} = \frac{\mu}{\mu_0} = \theta^n$$

From table 1 and Eq. (1) to (3), the reactions rates w_I, w_{II}, w_{III}, and w_{IV} are

$$\begin{aligned} w_I &= A\theta^{-2} k_I X_F X_H \\ w_{II} &= A\theta^{-2} k_{II} X_H (X_{CO} - L_{CO}\beta X_{H_2}/L_{H_2}) X_{H_2O}/X_{H_2} \\ w_{III} &= A\theta^{-2} k_{III} X_{O_2} X_H \\ w_{IV} &= A\theta^{-2} k_{IV} X_{O_2} X_H (1 - CX_H^2)/(1 + \Delta X_H) \end{aligned} \tag{17}$$

where $A = l\rho_0/(v_0 W_{N_2})$, $k_I = k_{R2} + k_{R3} + k_{R4} + k_{R5}$, $k_{II} = k_{9f}/K_3$, $k_{III} = k_5 C_M$, $k_{IV} = k_{1f}$, $\beta = (K_3/K_9)(X_{CO_2}/X_{H_2O})(L_{H_2}/L_{CO})$,

$$C = \frac{1}{FK_1K_2K_3^2}\frac{X_{H_2O}^2}{X_{H_2}^3 X_{O_2}}$$

$$\Delta = \frac{k_{1b} X_{H_2O}}{K_3 X_{H_2} (k_{2f} X_{H_2} + k_{4b} X_{H_2O})}$$

The value of F depends on the approximation which is adopted to describe the O-radical concentration. If O-radical is determined by Eq(2) or by Eq(4), F is defined by

$$F \equiv \begin{cases} [(k_{4b} X_{H_2O})/(k_{2f}) + X_{H_2}][(k_{4f} X_{H_2O})/(k_{2b} K_3) + X_{H_2}]^{-1} \\ 1, \end{cases}$$

if O-radical is determined by Eq(2) or by Eq(4), respectively.

Employing Eq.(4) insteady of Eq.(2) to evaluate the O-radical concentration, Δ is zero and $F = 1$, which eliminates the influence of reaction 4.

Equations. (7) to (16) satisfy the the boundary conditions:

$$U = 0, \quad V = 1, \quad \theta = 1, \quad X_{O_2} = X_{O_2 0}, \quad \text{and}$$

$$X_i = 0 \quad (i = F,\ H_2,\ H,\ CO,\ CO_2,\ H_2O), \qquad \text{at} \quad z = 0 \tag{18}$$

$$U = 0, \quad V = V_1, \quad \theta = \theta_1, \quad X_F = X_{F1}, \quad \text{and}$$

$$X_i = 0 \quad (i = O_2,\ H_2,\ H,\ CO,\ CO_2,\ H_2O), \qquad \text{at} \quad z = 1 \tag{19}$$

The momentum of the streams at the nozzle exits determine the location of the stagnation point z_s, which is given by the condition $V = 0$ and $dU/dz = 0$. The position of the flame z_f, where$X_F = X_{O_2} = 0$, is imposed by the hydrodynamic problem, by the fuel and oxidant Lewis numbers and by the fuel and oxidant concentrations upstream. Thereby, the diffusion flame position in the counterflow is $z_f = z_s \pm O(1/\sqrt{Pe})$.

The values to be used to perform the flame structure analysis are: flame temperature θ_f, flame position z_f, and fluxes of oxidant and fuel ,a_{O_2} and a_F, to the flame and the heat fluxes a_θ^- and a_θ^+ at the flame which are defined by:

$$a_{O_2} = \left.\frac{dX_{O_2}}{dz}\right|_{z=z_f^-}, \qquad a_F = \left.\frac{dX_F}{dz}\right|_{z=z_f^+}, \qquad a_\theta^- = \left.\frac{d\theta}{dz}\right|_{z=z_f^-}, \qquad \text{and} \qquad a_\theta^+ = \left.\frac{d\theta}{dz}\right|_{z=z_f^+}.$$

4. FLAME STRUCTURE AND EXTINCTION CONDITION

The analytical description of flames, diffusive and premixed types, starts considering an infinitely fast chemical reaction, known as Burke-Schumann's kinetic, which leads to an infinitely thin flame structure. This hypothesis represents well combustion problems because flames burn generally very fast. In spite of the drastic simplification that the Burke-Schumann's kinetic imposes, the model is able to determine all characteristics of the diffusion flame: flame temperature, flame position, fuel and oxidant consumptions, but it does not allow the determination of the conditions of flame extinction. The extinction analysis of diffusion flames demands a complete description of the structure of the flame which is imposed by the profile of the reaction rates of each species inside the flame. Since we are considering the kinetic mechanism of the n-heptane oxidation with four steps as shown by reaction from (I) to (IV), the rate-ratio asimptotics based on the difference among chemical rates is used to analyse the n-heptane diffusion flame structure.

The method of rate-ratio asimptotics was proposed by Peters and Willims (1987) and since then it has been constantly improved (Seshadri, 1996). Since its presentation is extense and already well known, only the results will be presented. The details of this asymptotic analysis are the same ones shown in the Card and Williams' (1992) article.

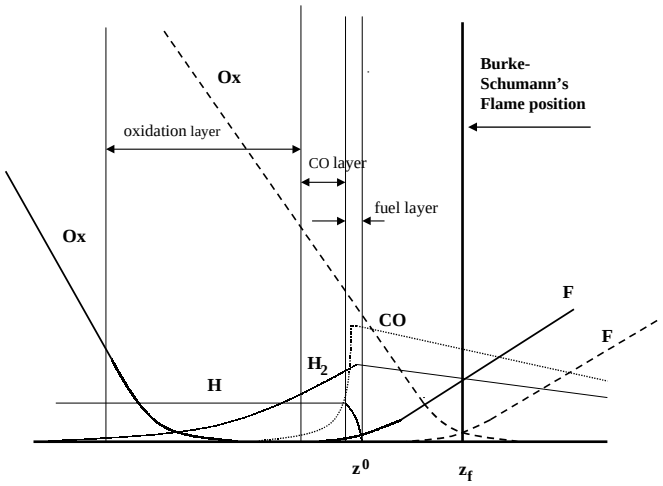

Figure 1: Flame temperature as function of the $(2\lambda|\nabla Z^*|^2)^{-1}$ for representative values, $L_F = 1.7$ and $L_{O_2} = 1.1$

A schematic picture of the structure of the diffusion flame is shown in Fig. 1. In this model we consider that the H-radical species is in steady state inside the flame and that the H-radical nonequilibrium layer, being much thinner than the fuel layer, is in the frozen-fuel side of the flame. Taking the Burke-Schumann's flame position as reference, the finite rate fuel layer is in the oxidant side of Burke-Schumann flame at the position $\xi^0_{O_2}$ and this is a characteristic of the n-heptane diffusion flame observed in previous analyses (Card and Williams, 1992). In the fuel layer the CO and almost all H_2 are produced. At the adjacent layer of the fuel layer, CO is completely consumed by reaction (II), producing CO_2 and more H_2. The H_2 boes by diffusion to the oxidation layer where it is completely consumed forming H_2O and the H-radical which is necessary to continue the reaction.

Following all these conditions the extinction of the n-heptane diffusion flame is determined by

$$\frac{32\rho_0^2 c_P l^2}{15 k_0 \theta^{0\ n+2}} \frac{L_F (F^0 K_1^0 K_2^0)^{1/2} K_3^0}{(\alpha a_F)^2 k_I^0 X^0_{H_2O}} \left(\frac{(22-\alpha)\bar{x}^0_{H_2}}{22} - \xi^0_{O_2}\right)^{5/2} \left(\frac{(22-\alpha) L_{H_2} \bar{x}^0_{H_2}}{11 L_{O_2}(1+\beta^f)}\right)^{3/2} \cdot$$

$$\cdot \left(1 - \frac{\varepsilon_{CO}}{\varepsilon_{O_2}} \frac{7 - \beta^0(15-\alpha)}{(22-\alpha)\bar{x}^0_{H_2}} \frac{1+\beta^f}{1+\beta^0}\right) \left(\frac{\theta^0 - \theta^f}{q\tilde{\Theta}^0}\right)^4 k^0_{1f} a^4_{O_2} = 1 \qquad (20)$$

$$\frac{2\rho_0^2 c_P l^2}{k_0 \theta_f^{n+2}} \left(\frac{22-\alpha}{11}\right)^2 \left(\frac{L^3_{H_2}}{L_{O_2}}\right)^{1/2} \frac{C^f_M (F K_1 K_2 K_3^2)^{f\,1/2}}{(1+\beta^f)^{3/2} X^f_{H_2O}} \left(\frac{\theta^0 - \theta^f}{q\tilde{\Theta}^0}\right)^4 k^f_5 a^2_{O_2} = 1 \qquad (21)$$

$$\bar{x}^0_{H_2} = 1.2949 + 0.31798\xi^0_{O_2} + 0.041927{\xi^0_{O_2}}^2 + 0.0024547{\xi^0_{O_2}}^3 + 5.1327\times 10^{-5}{\xi^0_{O_2}}^4 \qquad (22)$$

$$\tilde{\Theta}^0 + \frac{(1+\beta^f)(q_{III}+q_{IV}) + 2\beta^f q_{II}}{2(1+\beta^f)} \frac{(22-\alpha)a_{O_2}}{11 L_{O_2}} \bar{x}^0_{H_2} = \frac{a^-_\theta\, \xi^0_{O_2}}{q} \qquad (23)$$

The superscript 0 found in Equations (20) to (23) identifies the condition at the border of the oxidation layer and the superscrit f identifies the condition at the flame position

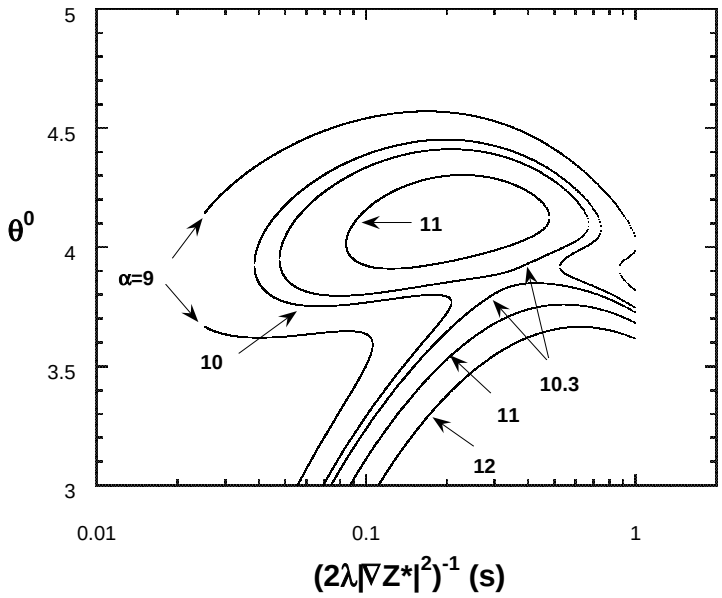

Figure 2: Flame temperature as function of the $(2\lambda|\nabla Z^*|^2)^{-1}$ for representative values, $L_F = 1.7$ and $L_{O_2} = 1.1$

specified by the Burke-Schumann's problem. The subscript 0 corresponds to the reference conditions of the flow. The variable $\tilde{\Theta}$ is the temperature in the oxidation layer.

The results of the analysis for the oxidation layer show that the concentration of H_2 at the border of the this layer does not change strongly with the number of moles of the H-radical. Thereby, it is possible to find an interpolation curve, represented by Eq. (22), of the H_2 concentration as a function of the position $\xi^0_{O_2}$.

The solution of Eqs. (20) to (23) for the temperature θ^0 is presented in Fig. 2. The case showed by this figure corresponds to the following conditions at the nozzles: inlet gases temperature 390K, heptane mass fraction 0.4, oxygen mass fraction 0.21 and the heptane, oxygen, CO_2 and H_2O Lewis numbers 1.7, 1.11, 1.39 and 0.83, respectively. Contrarily to what is observed in premixed flames, the "isola" behavior of the diffusion flames with the stretch occurs for weak states of the flame, in the range $10.3 < \alpha < 12$. For $\alpha > 12$, the isola desappears and also the extinction conditions, the solution becomes single. The upper branch of the isola and of other curves correspond to a stable solution, but the lower branch of the isola is unstable. The two turning points determine the extinction conditions. At the lowest turning point the extinction is caused by the radiative energy loss and at the highest point the extinction is caused by the diffusion of reactants through the flame.

Near the extinction points the problem presents three solutions, the third solution, like the first one, is stable. This extra stable solution has not been observed neither theoretically nor experimentally in diffusion flames before, so that the question is if it has a physical meaning or not. A fact that diminishes the credibility of this solution is its proximity to the turning point corresponding to the radiative extinction, meaning that the extinction at low stretch rate might not occur because the falling of the temperature between the two curves is not significantly large to extinguish the flame. This feature does not occur at the other turning point. From Fig. 2 it is also seen that the temperatures θ^0 at extinction in the diffusive and radiative regimes are very close, $\theta^0 \sim 4$.

Collecting data for the reciprocal of the scalar dissipation at extinction for radiative

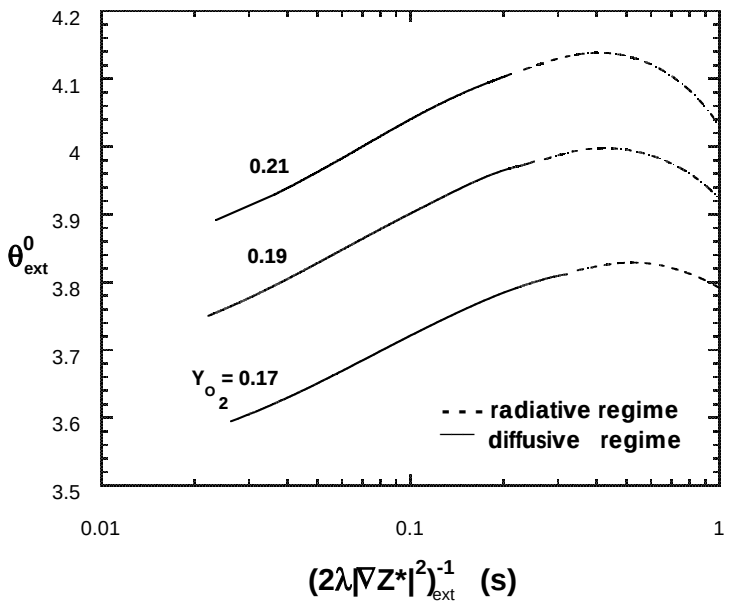

Figure 3: Temperature θ^0 in function of the reciprocal scalar dissipation $(2\lambda|\nabla Z^*|^2)^{-1}$ for the extinction condition.

and diffusive regimes for each value of α, the stable burning conditions for the stretched heptane diffusion flames is specified. Figure (3) shows the limits for the stable burning regime for three different compositions of air. It can be observed that for each composition of air, there is a maximum value of α beyond which the flame does not exist. At this maximum the radiation energy loss and the diffusion of reactants through the flame share the power to extinguish the flame. The dependence of the flame on H-radical is so strong that near this limit the combustion becomes incomplete and, thereby, the flame becomes wider, favoring the radiative energy loss; the combination of these two processes does does not allow the flame stabilization. Another fact that the figure exposures is the linear dependence of the reciprocal scalar dissipation on the oxygen mass fraction; the curves are very similar in shape, but they are only displaced one from the other.

5. CONCLUSION

It was analysed the influence of the number of moles of the H-radical α of the reduced kinetic mechanism on the stretched heptane diffusion flame. To avoid the hard task of determination of α, it is considered a free parameter in the model. It is seen that increasing the value of α, the diffusion flame becomes weaker and there is a limiting value above which the flame can not be stablished. Since the radiative energy loss is included in the model, it can be observed the radiative and diffusive regimes on the extinction process. Also, the search for solutions of the diffusion flames is extended to identify a second stable burn regime for the heptane flame.

Ackowledgment

This work was supported in part by the Conselho Nacional de Desenvolvimento Científico e Tecnológico - CNPq under the Grants 200554/87-5 and 300651/95-3.

REFERENCES

Bai, X.S., Seshadri, K., (1999), Rate-Ratio Asymptotic Analysis of Nonpremixed Methane

Flames, Combusiton Theory and Modeling, vol. 3, pp. .

Bollig, M., Pitsch, H., Hewson, J.C., Seshadri, K., (1996), Reduced n-Heptane Mechanism for Non-Premixed Combustion with Emphasis on Pollutant-Relevant Intermediate Species, Twenty-Sixth Symposium (Inernational) on Combustion, Combustion Institute, pp. 729-737.

Bui-Pham, M., Seshadri, K., (1991), Comparison betweedn Experimental Measurements and Numerical Calculations of the Structure of Heptane-Air Diffusion Flames, Combustion Science and Technology, vol. 79, pp. 293-310.

Card, J.M., (1993), Asymptotic Analisys for the Burning of n-Heptane Droplets Using a Four-Step Reduced Mechanism, Combustion and Flame, vol. 93, pp. 375-390.

Card, J.M., Williams, F.A., (1992), Asymptotic Analisys of the Structure and Extinction of Spherically Symmetrical n-Heptane Diffusion Flames, Combustion Science and Technology, vol. 84, pp. 91-119.

Card, J.M., Williams, F.A., (1992), Asymptotic Analisys with Reduced Chemistry for the Burning of n-Heptane Droplets, Combustion and Flame, vol. 91, pp. 187-199.

Dixon-Lewis, G., (1990), Structure of Laminar Flames, Twenty-Third Symposium (International) on Combustion, Combustion Institute, pp. 305-324.

Kee, R.J., Miller, J.A., Evans, G.H., Dixon-Lewis, G., (1988), A Computational Model of the Structure and Extinction of Strained, Opposed Flow, Premixed Methane-Air Flames, Twenty-Second Symposium (International) on Combustion, The Combustion Institute, Pittisburg, PA, pp. 1479-1494.

Keyes, D.E., Smooke, M.D., (1987), Flame Sheet Starting Estimates for Counterflow Diffusion Flame Problems, Journal of Computational Physics, vol. 73, pp. 267-288.

Law, C.K.,(1988), Dynamics of Stretched Flames, Twenty-Second Symposium (International) on Combustion, Combustion Institute, pp. 1381-1402.

Li, S.C., Williams, F.A., (1999), Experimental and Numerical Studies of Two-Stage Heptane Spray Flames, 37th AIAA Aerospace Sciences Meeting and Exhibit, AIAA paper 99-0211, Reno NV, Jan. 11-14.

Libby, P.A., (1998), Premixed Laminar Flames in Impinging Flows, Combustion Science and Technology, vol. 131, pp.345-379.

Libby, P.A., Smooke, M.D., (1997), The Computatrional of Flames in Stagnation Flows, Combustion Science and and Technology, vol. 127, pp. 197-211.

Olson, S.L., T'ien, J.S., (1987) A Theoretical Analysis of the Extinction Limits of Methane-Air Opposed-Jet Diffusion Flame, Combustion and Flame, vol. 70, pp.161-170.

Peters, N., and Williams, F.A, (1987), The Asymptotic Structure of Stoichiometric Methane-Air Flames, Combustion and Flame, vol. 68, pp. 185-207.

Rightley, M.L., Williams, F.A.], (1997), Structures of CO Diffusion Flames Near Extinction, Combustion Science and Technology, vol. 125, pp. 181-200.

Seshadri, K., (1996) Multisteps Asymptotic Analyses of Flame Structures, Invited Topical Review, Twenty-Sixth Symposium (International) on Combustion, pp. 1997-2006.

Seshadri, K., Peters, N., (1988) Asymptotic Structure and Extinction of Methane-Air Diffusion Flames, Combustion and Flame, vol. 73, pp. 23-44.

Seshadri, K., Peters, N.], (1990), The Inner Structure of Methane-Air Flames, Combustion and Flame, vol. 81, pp. 96-118.

T'ien, J.S., (1986) Diffusion Flame Extinction at Small Stretch Rates: The Mechanism of Radiative Loss, Combustion and Flame, vol. 65, pp.31-34.

Tsuji, H., 1982, Counterflow Diffusion Flames, Prog. Energy Combst. Sci., vol 8, pp. 93-119.